Journal of Pharmaceutical Sciences 114 (2025) 577–585

Contents lists available at ScienceDirect

Journal of Pharmaceutical Sciences

journal homepage: www.jpharmsci.org

Pharmaceutics, Drug Delivery and Pharmaceutical Technology

Complemental hard modeling in Raman spectroscopy: A case study on titanium dioxide-free coating in-line monitoring

René Brands, Jens Bartsch, Markus Thommes*

Laboratory of Solids Process Engineering, Department of Biochemical and Chemical Engineering, TU Dortmund University, 44227 Dortmund, Germany

ARTICLE INFO

Article history:
Received 22 July 2024
Revised 22 October 2024
Accepted 22 October 2024
Available online 23 November 2024

Keywords:
Pharmaceutical coating
Raman spectroscopy
Process analytical technology
Titanium dioxide-free coating
Spectral hard modeling

ABSTRACT

Tablets are coated for taste or odor modification, for modified release profiles or as a protective layer to increase the stability. Here, titanium dioxide is frequently added as a coating component due to its opaque properties. Furthermore, its Raman activity makes it an integral part of in-line monitoring models. However, due to the carcinogenic potential of titanium dioxide, calcium carbonate is utilized as a substitute, exhibiting similar opaque properties. Calcium carbonate tends to exhibit overlapped peaks with carbon hydrates in the Raman spectrum. Consequently, new models based on e.g. hard modeling are required instead of peak integration. In this study, tablets were coated with a coating including calcium carbonate. Partial Least Squares Regression (PLS) and Complemental Hard Modeling (CHM) were examined as feasible in-line monitoring approaches. Furthermore, two different measurement positions in the coater were compared, orthogonal and tangential with respect to the moving tablet bed. Cross-validation exhibited improved CHM performance with reduced RMSECV values of about 5 %. The prediction of the coating mass growth occurred comparable with RMSEP values in a similar range of 2–5 %. Despite this, the CHMs achieved improved performance with reduced training data quantity and quality. The different measurement positions indicated no process-relevant differences.

Introduction

Coating pharmaceutical tablets is an essential unit operation to improve taste, appearance and stability combined with enabling controlled release and protecting the Active Pharmaceutical Ingredient (API).[1,2] Traditionally, tablet coatings contain often titanium dioxide due to its opacity properties. However, with emerging health concerns, the pharmaceutical industry is currently switching to titanium dioxide-free coatings as it is considered to be potentially carcinogenic.[3–5] Consequently, the mostly separated titanium dioxide peaks in Raman spectra are no longer available for peak integration.[6] Calcium carbonate can serve as a substitute due to its similar opaque properties. However, it tends to exhibit interfering Raman peaks with hydrocarbon excipients like lactose and cellulose.[7] Therefore, robust in-line monitoring strategies based on titanium dioxide-free prediction models are necessary to ensure the quality and regulatory compliance of pharmaceutical tablet coatings.[8]

These in-line monitoring models provide real-time data about the process based on the implementation of Process Analytical Technologies (PAT).[9] The data obtained in real time can be utilized for real-time release testing and thus replace the time-consuming off-line testing of samples.[10] Furthermore, the acquired data has the potential to be integrated into control regimes and thus contribute to the digitalization of pharmaceutical processes.[11] Here, the spectroscopic methods that are non-invasive and non-destructive and provide real-time data with high accuracy are particularly suitable.[12]

In this context, near infrared spectroscopy (NIR) is known for its ability to provide chemical and physical information. This makes NIR spectroscopy a suitable in-line monitoring tool for evaluating of the coating thickness and composition of the coating material.[13,14] Nevertheless, NIR requires considerable high calibration effort for molecule-specific applications. Furthermore, humidity can also be monitored as an additional critical quality attribute for moisture sensitive materials.[15] Terahertz time-domain imaging provides information on physical properties and is a promising tool for precise endpoint determination in tablet coating for coating thicknesses and is independent of the coating and tablet core formulation.[16,17] On the other hand, optical coherence tomography (OCT), enables critical quality attributes in-line monitoring of coating thickness, variability and roughness making OCT to a valuable aid in detecting defects in tablet coating as long as the refractive index difference can be determined.[18,19] Although, OCT does not work if the coating formulation contains inorganic pigments.[20] A combination of X-ray

* Corresponding author.
E-mail address: professors.fsv.bci@tu-dortmund.de (M. Thommes).

https://doi.org/10.1016/j.xphs.2024.10.044

fluorescence spectroscopy and a Monte Carlo simulation was used to determine the coating thickness.[21] However, despite the advantages of each PAT technology, the specific requirements of tablet coating processes, particularly for monitoring coating mass on tablets and determining coating endpoints, Raman spectroscopy was frequently implemented. It is characterized by a molecular specificity and high sensitivity.[22–25]

In order to obtain quantitative information from the spectral data, models must be developed. In this context, Partial Least Squares Regression (PLS-R) is a well-established statistic method for building predictive models based on Raman spectroscopy data.[22,26,27] It enables the extraction of relevant information from complex data sets and links between the spectral Raman information and critical quality attributes of tablet coatings like coating thickness and coating mass growth.[28] However, the performance of PLS-R can be limited by multicollinearity and overfitting caused by the incorrect selection of a PLS-R rank.[29,30] Furthermore, nonlinearity can be only modeled to some extent.[31] Therefore, an alternative will be considered in this study.

Here, spectral Hard Modeling (HM) should be considered as an alternative approach that is capable to compensate the observed limitations of PLS-R.[32] The principle of Hard Modeling (HM) consists of the construction of mathematical models in form of phenomenological motivated non-linear models representing peak functions (i.e. pseudo-Voigt type), so called Hard Models, which are integrated, superimposed and weighted.[33] In contrast to traditional statistical regression methods, HM directly incorporates physical and chemical principles underlying the Raman spectral data and thus contributes to a more mechanistic interpretation.[34] Additionally, the amount of data required for calibration is significantly reduced compared to a PLS-R.[35] Complemental Hard Modeling (CHM) extends this approach. Here, only a single spectrum of the mixture and the spectra of the pure components are required as input data for the calibration. First Hard Models are combined to develop a mixture model, which is subsequently expanded by an additional Hard Model for the unknown component in the mixture spectrum.[31,36,37]

The objective of this study is to compare well-established PLS-R with the comparatively new Complemental Hard Modeling for in-line monitoring of titanium dioxide-free tablet coatings. In particular, the study focuses on evaluating the performance of these models for prediction of the mass growth of the coating material. In addition, the influence of the probe position on the models was investigated. For this purpose, the probe was implemented at two different measurement positions, at the nozzle arm measuring orthogonal and in the back wall of the coater measuring tangential to the tablet bed.

Material and methods

Tablet cores

The tablet formulation consisted of 50 wt% paracetamol (Compap L, Mallinckrodt Pharmaceuticals, Staines-upon-Thames, Ireland), 44 wt% microcrystalline cellulose and colloidal silicon dioxide pre-blend (Prosolv SMCC 90, JRS Pharma, Rosenberg, Germany), 5 wt% crospovidone (Kollidon CL, BASF, Ludwigshafen, Germany) and 1 wt% magnesium stearate (Ligamed MF-2-V, Peter Greven, Bad Münstereifel, Germany). Tableting was executed on a rotary tablet press (XL 100, Korsch, Berlin, Germany) equipped with ten 8 mm diameter R9 punches. A main compression force of 10 kN and a tablet mass of 220 mg were set at a tableting speed of 60 rpm.

Coating suspension

The titanium dioxide free coating suspension consists of 85 wt% demineralized water and 15 wt% coating material (Aquarius prime TF pink, Ashland, Covington, USA), which contains calcium carbonate as a Raman-active substance, hydroxypropylmethylcellulose, polyethylene glycol and yellow, red and black iron oxide. For the suspension, 2.4 kg powder were dispersed in 13.6 kg water using a propeller stirrer (IKA-Werke, Staufen, Germany) and the suspension was stirred continuously during the coating process.

Coating process

A total of six batches were coated, three for each of the two measurement positions. For each individual run, 10 kg tablets were loaded into the semi-continuous coater KOCO 25 (L.B. Bohle, Ennigerloh, Germany). Initially, the tablets were warmed up with warm air. Six type 970 1 mm nozzles (Düsen-Schlick, Untersiemau, Germany) at a distance of 10 cm to the tablet bed were utilized for dispersing the coating suspension. During the process, the tablets were coated with a total of 650 g of coating material. In order to maintain a constant spray rate and a constant coating mass growth, the change in weight of the coating suspension was monitored. After the coating process, the spray nozzles were switched off and the tablets were dried at a reduced drum speed. Finally, the tablets were cooled down and discharged from the coater. The process parameters during the coating process are shown in Table 1.

Off-line coating mass determination

Samples of the coated tablets were manually taken every three minutes during the coating process via the sample valve of the machine. Subsequently, for each sampling point in time 60 tablets were taken and divided into three groups of 20 tablets each and the total mass was determined via a lab scale (MCE224S Cubis, Sartorius, Goettingen, Germany). The average mass growth per tablet was calculated considering the number of tablets per sampling. Subsequently, the total coating mass increase was then calculated for the entire mass of tablets in the coater.

Raman spectroscopy

The Raman spectra were measured in-line using a Raman Spectrophotometer (Process Guardian, Tornado Spectral Systems, Mississauga, Canada) with a special probe (Hudson 785, Tornado Spectral Systems, Mississauga, Canada). The dimensions of this Raman probe are 5.5 × 4.5 × 2.6 cm. This non-contact probe in combination with a large sport optic allows the measurement of areas with a spot diameter of 4 mm. The device uses a 785 nm laser for the excitation of the

Table 1
Process parameters for the individual process steps during the coating process.

Process step	Process time [min]	Pan speed [rpm]	Spray rate [g/min]	Atomization/ Pattern air [bar]	Inlet air volume [Nm^3/h]	Inlet air temperature [°C]
Warm up	5	2	–	–	550	68
Coating	65	17	65	1.3 / 1.0	550	68
Drying	70	5	–	–	550	68
Cooling	75	5	–	–	550	22

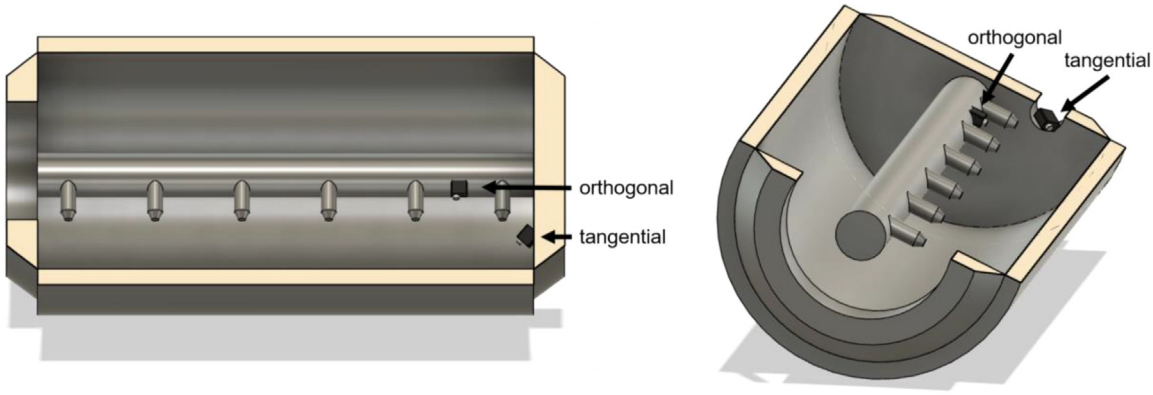

Fig. 1. Schematic illustration of the Raman probe positions in the coater.

Raman signal. Raman spectra from 200 to 3300 cm^{-1} with 1 cm^{-1} resolution were obtained, processed with a cosmic ray filter, y-axis and dark correction and average spectra were evaluated over 15 spectra. The exposure time was adjusted according to the measurement position. Particular two different measurement positions were selected and compared to each other. Here, the probe was installed in the back wall of the coater and measures tangential to the tablet bed and in the other position, the probe was installed on the nozzle arm and measures orthogonal to the tablet bed (Fig. 1). These different measuring positions resulted in different exposure times and measuring frequencies (Table 2) in order to achieve comparable signal intensities. Compressed air streams were used to keep the optics free of fine dust and thus enable continuous measurements.

Data analysis methods

For the calibration model and the prediction of the coating mass, the spectra were pretreated and two different model types were developed by using the PEAXACT 5 software (S-PACT, Aachen, Germany). First, a statistical model based on Partial Least Squares Regression (PLS-R) and secondly, a mechanistic model based on Complemental Hard Modeling (CHM) were developed. In both cases, this was performed for each of the two measurement positions. Therefore, two of the three batches per measurement position were randomly selected for training purposes and one batch was used as a test data set. Additionally, cross-validations were performed as leave-one-batch-out.

Spectra pretreatment

The spectra were preprocessed with a baseline correction in terms of rubber band correction by manually setting additional baseline points at 357, 424, 487, 666, 696, 772, 1061, 1140, 1299, 1423 and 1583 cm^{-1} to remove the spectral background. Additionally, the global range was adjusted to 200 – 1750 cm^{-1} as the primary spectrum differences are recognizable in this range. Subsequently, a peak height normalization was performed in relation to the largest peak of the tablet core, which can be assigned to the paracetamol, in order to highlight the changes caused by the coating.[38]

Table 2
Comparison of the two different measurement positions and the corresponding measurement setups.

Position	Exposure time [s]	Measurement frequency [s^{-1}]	Distance [cm]
tangential	2.0	0.033	9
orthogonal	0.9	0.074	11

Partial least squares regression

Calibration models based on PLS Regression were developed. For modeling, all pretreated spectra of the training data sets were correlated with the amount of applied coating material. The rank selection of the corresponding PLS models were based on physically reasonable effects e.g. peak increase with increasing coating material or peak broadening in order to avoid overfitting. Therefore the PLS loadings were considered.

Complemental hard modeling

For CHM, only a single spectrum of the mixture that contains the known and unknown materials and the spectra of the remaining pure components are required as input. In this particular case, the tablet core represents the known pure substance and the tablet coating represents the unknown component. For the spectrum of the uncoated tablet, the first spectrum of the measurement series was used, in which no coating suspension was sprayed. Here, the model-relevant spectral range was adjusted to 1065 to 1145 cm^{-1}, according to the $CaCO_3$ Raman bands. Initially, spectral peak functions are fitted to the spectral structure of the tablet core to model its spectral contribution (Fig. 2). In this particular case, three peak functions must be fitted, representing the two microcrystalline cellulose peaks and the one paracetamol peak, resulting in the Hard Model of the tablet core. Subsequently, the $CaCO_3$ is modeled from the spectrum of a coated tablet by an extra peak function, which represents the signal contribution (component weight) of the coating material that is finally translated into coating progress by a calibration with samples of known carbonate content. For this purpose, the spectra belonging to a sample pull with a coating mass increase determined off-line using the reference method were selected and correlated to the component weight. When analyzing unknown samples, the model is first least-squares fitted to the spectrum through adjustment of the weight of the components, the baseline and the peak parameters, and then using the component weight to determine the amount of carbonate coated.

Model performance assessment

Quality parameters were used to compare the performance of the models. For this purpose, the calibration was evaluated using the coefficient of determination (R^2). However, R^2 is interpreted differently in a statistical model (PLS-R) and a mechanistic model (CHM). In statistical models, the R^2 describes the explained variance, whereas in mechanistic models it represents the collinearity factor. Furthermore, the corresponding data sets were cross-validated between different batches of the training data set and the root mean squared errors of cross validation (RMSECV) were determined. The prediction quality was determined using the test data sets, whereby

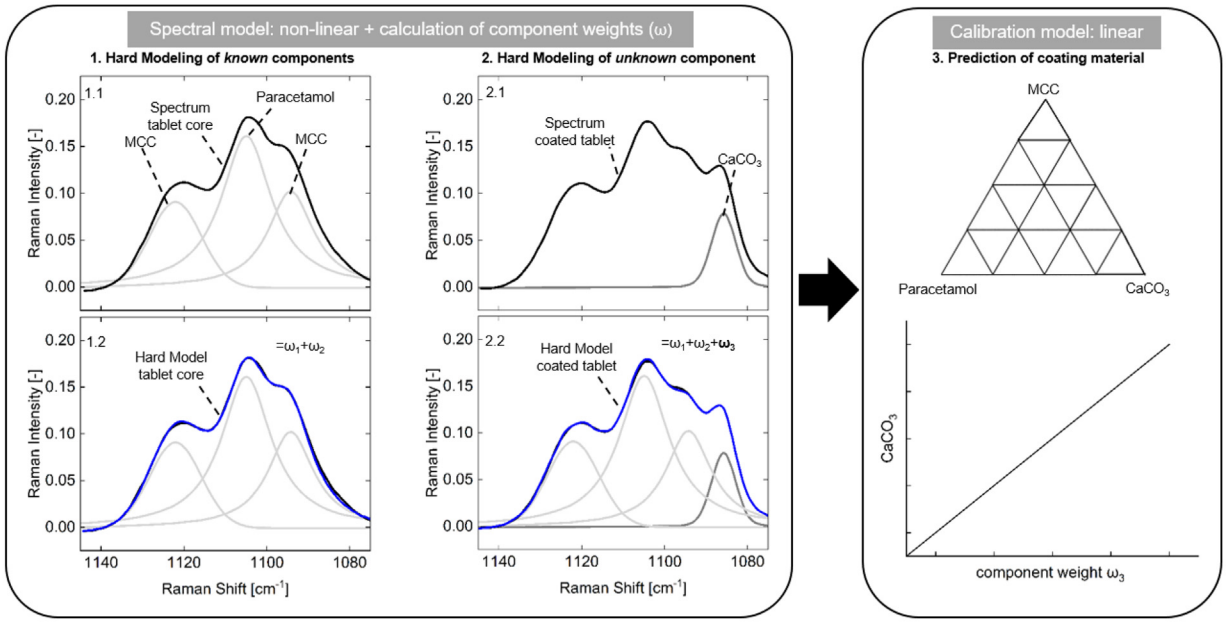

Fig. 2. Schematic representation of Complemental Hard Modeling with non-linear spectral model (left) and linear calibration model (right) adapted according to[31].

the root mean squared errors of prediction (RMSEP) were determined. Here, low RMSECV and RMSEP and high R^2 values are preferred. Percentage root mean squared errors are given in relation to the applied coating mass to improve comparability.

Results and discussion

Off-line coating mass determination

First investigations dealt with the tablet mass increase based on coating (Fig. 3). For this purpose, samples were taken every three minutes and the mass increase was evaluated according to 2.4. An average mass increase was calculated from the triplicate measurements and the applied coating mass was calculated in relation to the total tablet mass in the coater. Over all, six batches were coated. Batches 1.1 to 1.3 were used for the tangential measurement position and batches 2.1 to 2.3 for the orthogonal measurement position. The tablet mass increases linear over time for all batches as coating material is applied with a continuous flow rate (Fig. 3). After one hour, approximately 8 mg/cm^2 of coating material was applied to each tablet. Moreover, the corresponding slopes representing the mass increase rate are overall within similar ranges. Therefore, the coating process appears to be consistent across all batches and repeatable.

Spectra pretreatment

The raw spectra presented in Fig. 4 (left) highlight a baseline shift, which increases at lower Raman shifts. At the same time, the number of identifiable peaks increases. The signal intensity decreases during the coating process with increasing coating mass on the tablets. However, the additional peaks from the coating cannot be spotted easily. Thus, the raw spectra highlights information about the tablet core and obscures information about the coating material. Generally, characteristic triplet Raman bands for paracetamol are apparent at approximately 1500 to 1700 cm^{-1}.[38] Furthermore, the Raman bands for microcrystalline cellulose are recognizable at approximately 380 and 1096 cm^{-1}.[7] However, the spectral changes associated with the coating are revealed by a spectral pretreatment that includes baseline and global range adjustment and peak height normalization to the highest tablet core peak (Fig. 4, right).

Calcium carbonate as a Raman-active component of the coating shows characteristic vibrations. In agreement to the literature,[39] Raman bands are observable at ~281 cm^{-1} and ~1437 cm^{-1}, while in particular the vibration at ~1087 cm^{-1} is apparent as a shoulder on the core signal. Furthermore, this Raman band at 1087 cm^{-1} exhibits a direct correlation between Raman intensity and coating mass (Fig. 4, right, zoom).

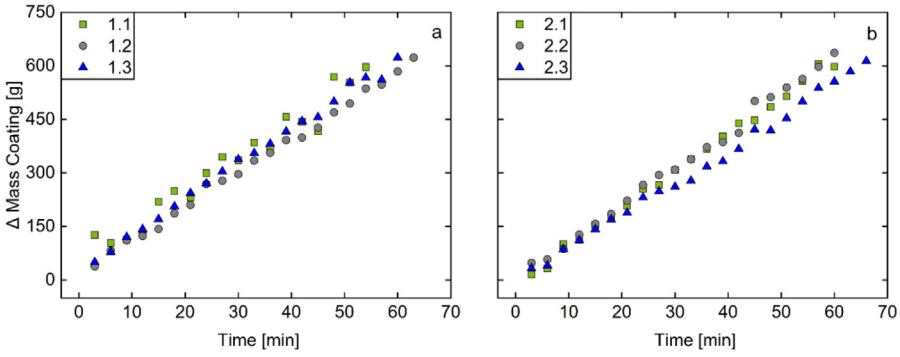

Fig. 3. Representation of the mass increase during the coating process over time for the tangential measurement position (left, a) and the orthogonal measurement position (right, b), including the three batches carried out for each measurement position.

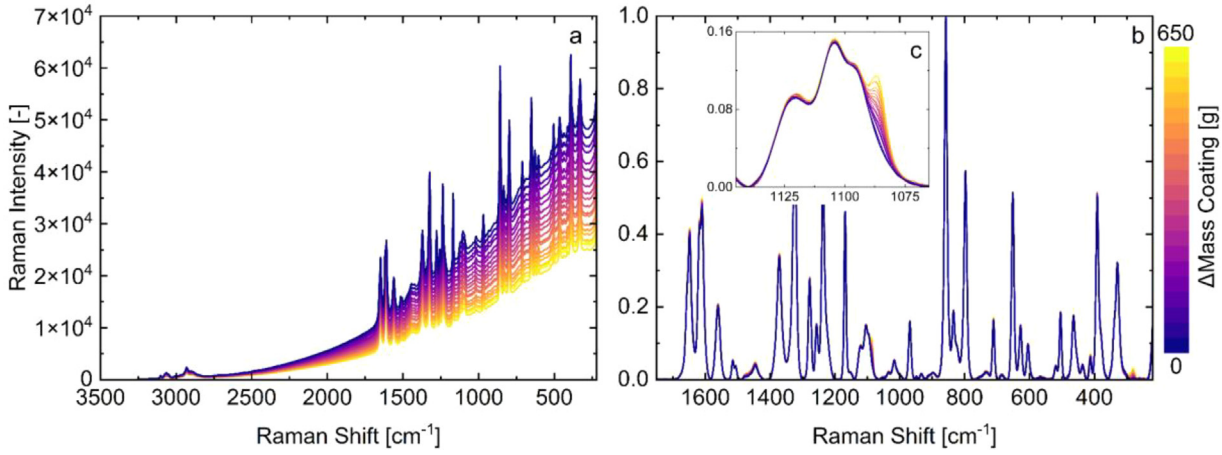

Fig. 4. The raw spectra without pretreatment (left, a) and the spectra after pretreatment (right, b), exemplary shown for batch 2.1 in orthogonal measurement position. Additionally spectral range from 1065 to 1145 cm^{-1} with correlation Raman intensity and mass of coating material at 1087 cm^{-1} (c).

Model evaluation

Partial least squares regression

For each measurement position, a PLS-R was developed. The PLS ranks were selected to ensure that the model quality was maximized in terms of sufficient R^2, RMSECV and RMSEP and the rank is physically explainable. For this purpose, the loadings of the PLS-Rs were considered (Fig. 5). Here, the loadings one up to three primarily represent the peak increase (rank 1) due to the coating and the peak broadening (rank 2–3).

It can be observed for both models that the model quality increases with increasing the rank, which can be verified by a decrease in RMSECV and RMSEP and an increase in R^2. Based on the loadings, higher ranks cannot be justified, as no relation between attributes and physics can be recognized. In order to avoid overfitting by selecting too high ranks, any ranks higher than three were excluded.

For the tangential position PLS-R, the highest model performance was achieved at a PLS rank of 2. The calibration model is sufficient with an R^2 of 0.98 and the coating mass prediction is sufficient with a minimum value for the RMSEP of 2.66 % (Table 3). At this rank, however, the RMSECV is still high with 17.09 %. This was attributed to the fluctuations in batch 1.1 (Fig. 3). Consequently, the two training data sets differ more in comparison to the other measurement position. This leads to increased RMSECV values in the cross-validation. In the case of Raman spectroscopy, peak shifting or broadening/narrowing may occur, which could act as a limiting factor for this statistical PLS-R, potentially interfering with the consistency of the data patterns that PLS-R relies on for accurate predictions. However, the RMSEP is considered to be the most important evaluation parameter for the application and prediction of the mass increase of the coating, as it describes the deviations of the predicted values from the true values. Therefore, rank 2 was selected for the tangential probe alignment.

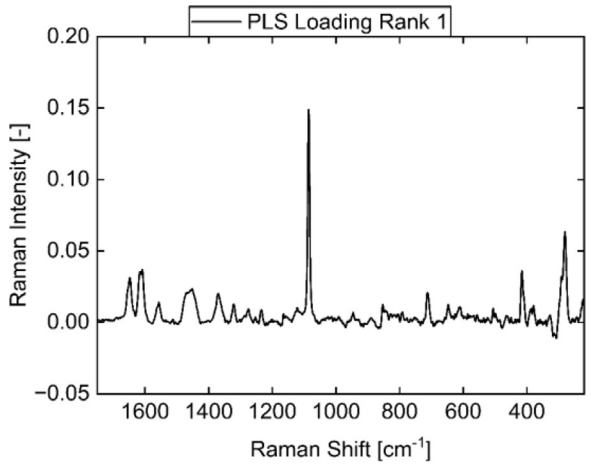

Fig. 5. PLS loading for rank 1 exemplary for the tangential measurement position.

A similar trend can be observed in the PLS-R for the probe with orthogonal alignment. With increasing the rank, the model quality increases. Therefore, rank 3 was chosen for the orthogonal position PLS-R. RMSEP, RMSECV and R^2 are suitable with 4.61 %, 5.56 % and 0.99.

The PLS-Rs are shown in Fig. 6, indicating the training samples and test samples. The calibration model of the tangential measurement position indicates a comparatively lower model quality in terms of the R^2 compared to the model of the orthogonal measurement position (Table 3). In Fig. 6, deviations of the training samples are more apparent for the tangential measurement position compared to the orthogonal measurement position. This can be attributed to the inherent fluctuation in the tablet bed height during the coating process and the different measurement spot positions of the two measurement positions.[40] Thus, depending on the position of the tablets in the coater and the corresponding Raman probe position, different tablet speed profiles and different tablet slipping behavior in terms of avalanches are expected. However, the predictive performance of the models is in reverse order. The PLS-R for the tangential measurement position indicates a higher model quality in terms of RMSEP compared to the PLS-R for the orthogonal measurement position. This conclusion relates to the data set presented in this study. In order to finally differentiate between the two measurements positions with regard to model performance, larger data sets are required. Nevertheless, both models are considered to be sufficient with regard to the requirements for a predictive model as they are characterized by RMSEP values of less than 5 %. Moreover, these model evaluation parameters are comparable to those of other PLS-Rs for pharmaceutical coating applications in the literature.[22]

Table 3
Model evaluation parameters for PLS models and probe measurement positions.

	R^2 [-]	RMSECV [%]	RMSEP [%]
tangential	0.98	17.09	2.66
orthogonal	0.99	5.56	4.61

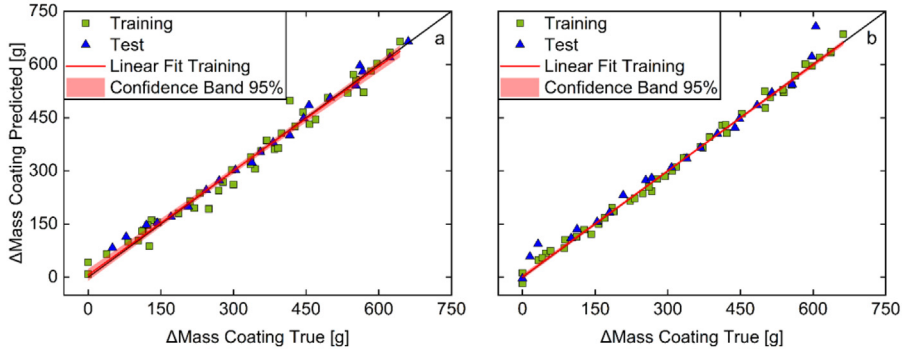

Fig. 6. Presentation of the PLS-R for both measurement positions, left tangential measurement position (a) and right orthogonal measurement position (b), with training and test samples.

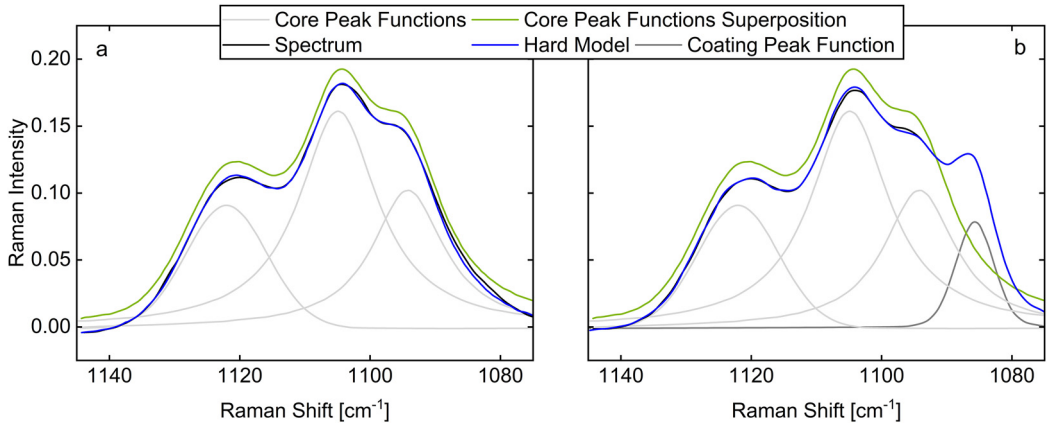

Fig. 7. Tablet core Raman spectrum (black) with tablet core Hard Model (blue) including three peak functions (light grey) for the tablet core (left, a) and final coated tablet spectrum (black) with Complemental Hard Model (blue) including three peak functions for the tablet core(light grey) and one peak function for the coating material (grey) (right, b), both exemplarily shown for batch 2.1.

Complemental hard modeling

In accordance with the procedure described in 2.7.3, separate CHMs were developed for each of the two measurement positions. Initially, pure component Hard Models were developed for the tablet core (Fig. 7, left). The peaks at 1096 cm^{-1} and 1132 cm^{-1} were attributed to microcrystalline cellulose (ν(COC)) and the peak at 1109 cm^{-1} to paracetamol ($\delta_{in\text{-}plane}$(HCC), ν(CNC), $\delta_{in\text{-}plane}$(HOC)).[7,38,41] Each of these consists of three peak functions describing the spectral response of the tablet core. Based on the residuals (<0.003) the agreement with of the Hard Model and the spectral response of the tablet core and thus the quality are considered to be sufficient.

Subsequently, the core Hard Models were transferred to the spectrum of coated tablets and complemented with a peak function for the calcium carbonate peak at 1087 cm^{-1} to capture the spectral information of the coating material (Fig. 7, right). The resulting CHMs exhibit high agreement with the corresponding spectrum of coated tablets, indicated by low residual values (<0.002) (Fig. 7, right). This applies to the CHMs for both positions.

The calibration model for the orthogonal measurement position has an increased R^2 compared to the tangential measurement position (Table 4), which can also be observed with respect to the deviations of the samples from the parity line (Fig. 8). Here, larger deviations of the training samples are apparent, especially in the range from 200 to 500 g of applied coating material. This is consistent with the data of mass increase over time (Fig. 3), where batch 1.1 exhibits increased process fluctuations. However, according to the cross-validation the CHM for the tangential measurement position has a higher model quality in terms of RMSECV but if the range is included, both RMSECV values can be considered as comparable. Thus, a higher capability to handle the interbatch variability in the prediction of coating mass grow during cross-validation is indicated for CHM in comparison to PLS-R. In comparison to the CHM for the orthogonal measurement position, the predictive power of the CHM for the tangential measurement position is characterized by larger deviations of the test samples and higher RMSEP value. This can be attributed to the fluctuation in the tablet bed described previously, which is of different magnitude for the two measurement spots. Consequently, the orthogonal measurement position model is preferable, taking into account that the training data for the tangential measurement position was comparatively inferior. Accordingly, further studies must be carried out with larger data sets in order to differentiate between the two measurement positions in terms of model performance. Based on the data presented in this study, both models can be classified as sufficient.

Table 4
Model evaluation parameters for CHM models and probe measurement positions.

	R^2 [-]	RMSECV [%]	RMSEP [%]
tangential	0.97	4.68	4.37
orthogonal	0.99	5.45	2.77

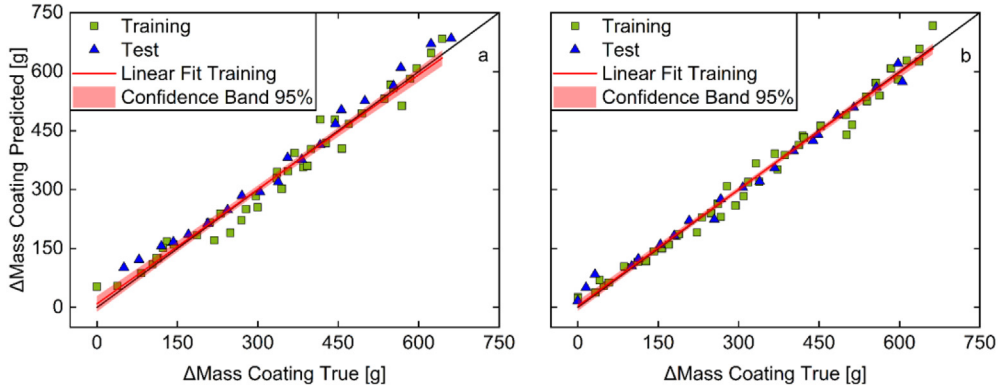

Fig. 8. Presentation of the CHM for both measurement positions, left tangential measurement position (a) and right orthogonal measurement position (b), with training and test samples.

Table 5
Model evaluation parameters for both model types based on training data batch 1.1 or 1.2.

		R^2 [-]	RMSECV [%]	RMSEP [%]
Training data batch 1.1	PLS	0.99	5.90	16.08
	CHM	0.95	7.01	5.98
Training data batch 1.2	PLS	0.99	5.91	12.63
	CHM	0.97	4.77	4.37

Model performance with respect to training data quantity and quality

The analysis of data with comparatively reduced quantity and quality was performed separately. Batches 1.1 and 1.2 were used as individual training data sets to predict batch 1.3. Compared to the models trained with the combined data of batches 1.1 and 1.2, the model evaluation parameters were generally reduced (Table 5). Similarly, it can be observed that the CHMs are characterized by decreased R^2 values compared to the PLS-Rs, 0.95 and 0.97 to 0.99 and 0.99. Considering the quantity of data for the respective calibration model, the R2 values can be classified as comparable in the overall context. However, the CHMs are superior to the PLS-Rs in terms of RMSEP, 5.98 % and 4.37 % to 16.08 % and 12.63 %. Generally, the models based on batch 1.1 as training data are characterized by a lower model quality than those with training data based on batch 1.2. This can be attributed to the general structure of CHMs as Hard Models. CHMs allow for improved coverage of spectral information and prediction of coating mass, even when peak position and width or data quality and quantity vary. In general, the CHMs perform better with reduced training data quantity and quality to predict the coating mass compared to the PLS-R. This is to be expected, since spectral Hard Modeling does not require a broad data set that fulfills all statistical requirements, but exploits the physical behavior of spectra when the chemical composition of a sample changes.[35]

In-line monitoring performance

The test batch spectra of the orthogonal measurement position were utilized to demonstrate the potential model-based in-line monitoring (Fig. 9) of the coating process over time. Here, measurement position two was selected as it is considered to be preferable based on the previous results. For this purpose, the two models developed, consisting of CHM and PLS-R for the orthogonal measurement position, were utilized to predict the coating mass increase based on the spectra data of batch 2.3. All available spectra were included, rather than just the ones that matched the sampling as in the model development. The overall spraying time was 60 min leading to a mass increase of roughly 600 g coating material on the tablet cores, which is observable in all experiments. The mass increase is determined for the total tablet mass in the coater. In general, an increase in the coating mass over time can be observed for both models. However, the models overestimate the coating mass applied at minute 60. The PLS model overestimates the applied coating mass by 6.5 % and the CHM overestimates the applied coating mass by 5.9 %. Despite this, the in-line predicted coating mass is in agreement with the off-line weight measurement. In conclusion, both models predict the increase in coating mass sufficiently well.

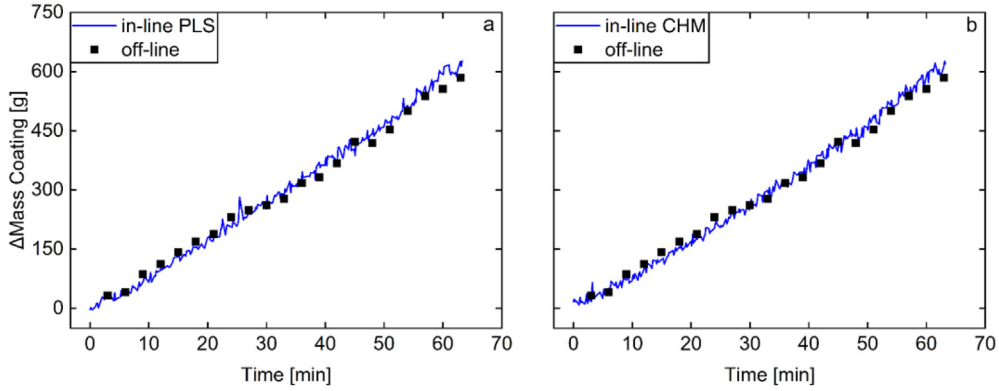

Fig. 9. The in-line monitored coating mass increase predicted on the basis of the models and off-line measurements are shown over the coating time. Results from PLS-R are shown on the left (a) and CHM on the right (b).

Conclusion

In this study, for the first time in-line monitoring methods for titanium dioxide-free coatings based on caclium carbonate as a substitute were developed utilizing Raman spectroscopy. For this purpose, tablets were coated in a KOCO 25 semi-continuous coater with a coating containing calcium carbonate. Here, two different Raman probe measurement positions in the coater were compared. Furthermore, two different model types were developed and compared in terms of model evaluation parameters, including statistical PLS-Rs and mechanistic CHMs. Additionally, the developed models were utilized to monitor the coating mass growth in-line based on the spectral data.

In general, the performed cross-validations indicate a higher model quality of the CHMs. The prediction models are comparable and have RMSEPs of less than 5 %. Nevertheless, the CHMs performed better with reduced data quality and data quantity, i.e. only one training data set used, indicated by comparable lower RMSEPs. This was attributed to the mechanistic structure of CHMs, achieved by solving least squares problems and adjusting component weights. Overall, it could be demonstrated that the developed models and their model performance are comparable to models based on titanium dioxide.

The tangential and the orthogonal measurement positions are different in terms of their exposure time and the resulting measurement frequency. Taking the process duration into account, both measuring frequencies are sufficient. The model evaluation parameters are better for the orthogonal measurement position compared to the tangential measurement position. Given the potential influence of data quality on the decision between the two measurement positions, further studies utilizing larger data sets are required to provide a more robust conclusion. In conclusion, it could be demonstrated that PLS as well as CHM are suitable for the endpoint detection of a titanium dioxide-free coating and provide real time data about the process that can be used for real-time release testing and digitalization.

Funding

The work was supported by the German Research Foundation [Grant SPP2364].

Declaration of competing interests

The authors declare the following financial interests/personal relationships which may be considered as potential competing interests:

Rene Brands reports financial support was provided by German Research Foundation SPP2364.

Acknowledgments

The authors acknowledge L.B. Bohle for providing the process equipment (i.e. KOCO 25 coater), S-PACT for support with the modeling, Tornado Spectral Systems for providing the Raman spectrophotometer, Prof. Dr. Freund for providing the PEAXACT software and Ashland for providing Aquarius prime TF pink.

Supplementary materials

Supplementary material associated with this article can be found in the online version at doi:10.1016/j.xphs.2024.10.044.

References

1. Zaid AN. A comprehensive review on pharmaceutical film coating: past, present, and future. *Drug Des Devel Ther*. 2020;14:4613–4623.
2. Seo K-S, Bajracharya R, Lee SH, Han H-K. Pharmaceutical application of tablet film coating. *Pharmaceutics*. 2020;12.
3. Radtke J, Wiedey R, Kleinebudde P. Alternatives to titanium dioxide in tablet coating. *Pharm Dev Technol*. 2021;26:989–999.
4. Lawrence S, James WA, Stewart S. 2023 APS Special Issue. *British J Pharm*. 2023;8.
5. Baan R, Straif K, Grosse Y, Secretan B, El Ghissassi F, Cogliano V. Carcinogenicity of carbon black, titanium dioxide, and talc. *Lancet Oncol*. 2006;7:295–296.
6. Kim B, Woo Y-A. Coating process optimization through in-line monitoring for coating weight gain using Raman spectroscopy and design of experiments. *J Pharm Biomed Anal*. 2018;154:278–284.
7. Queiroz ALP, Kerins BM, Yadav J, et al. Investigating microcrystalline cellulose crystallinity using Raman spectroscopy. *Cellulose*. 2021;28:8971–8985.
8. Blundell R, Butterworth P, Charlier A, et al. The role of titanium dioxide (E171) and the requirements for replacement materials in oral solid dosage forms: an IQ consortium working group review. *J Pharm Sci*. 2022;111:2943–2954.
9. FDA. Guidance for industry PAT - a framework for innovative pharmaceutical development. *Manufac Qual Assur*. 2004.
10. Markl D, Warman M, Dumarey M, et al. Review of real-time release testing of pharmaceutical tablets: state-of-the art, challenges and future perspective. *Int J Pharm*. 2020;582:119353.
11. Hole G, Hole AS, McFalone-Shaw I. Digitalization in pharmaceutical industry: what to focus on under the digital implementation process? *Int J Pharmac*. 2021;3:100095.
12. K.A. Bakeev, Process Analytical technology: Spectroscopic tools and Implemented Strategies For the Chemical and Pharmaceutical Industries /edited by Katherine A. Bakeev, 2nd ed., Wiley-Blackwell, Oxford, 2010.
13. Avalle P, Pollitt MJ, Bradley K, et al. Development of Process Analytical Technology (PAT) methods for controlled release pellet coating. *Europ J Pharm Biopharm*. 2014;87:244–251. V.
14. Gendre C, Genty M, Boiret M, et al. Development of a process analytical technology (PAT) for in-line monitoring of film thickness and mass of coating materials during a pan coating operation. *Europ J Pharm Sci*. 2011;43:244–250.
15. Knop K, Kleinebudde P. PAT-tools for process control in pharmaceutical film coating applications. *Int J Pharm*. 2013;457:527–536.
16. May RK, Evans MJ, Zhong S, et al. Terahertz in-line sensor for direct coating thickness measurement of individual tablets during film coating in real-time. *J Pharm Sci*. 2011;100:1535–1544.
17. Russe I-S, Brock D, Knop K, Kleinebudde P, Zeitler JA. Validation of Terahertz coating thickness measurements using X-ray microtomography. *Mol. Pharm.*. 2012;9:3551–3559.
18. Sacher S, Peter A, Khinast JG. Feasibility of in-line monitoring of critical coating quality attributes via OCT: thickness, variability, film homogeneity and roughness. *Int J Pharm*. 2021;3:100067.
19. Markl D, Hannesschläger G, Sacher S, Leitner M, Khinast JG. Optical coherence tomography as a novel tool for in-line monitoring of a pharmaceutical film-coating process. *Europ J Pharm Sci*. 2014;55:58–67.
20. Lin H, Dong Y, Markl D, Zhang Z, Shen Y, Zeitler JA. Pharmaceutical film coating catalog for spectral domain optical coherence tomography. *J Pharm Sci*. 2017;106:3171–3176.
21. Giurlani W, Berretti E, Innocenti M, Lavacchi A. Coating thickness determination using X-ray fluorescence spectroscopy: monte carlo simulations as an alternative to the use of standards. *Coatings*. 2019;9:79.
22. Barimani S, Kleinebudde P. Evaluation of in-line Raman data for end-point determination of a coating process: comparison of science-based calibration, PLS-regression and univariate data analysis. *Europ. J. Pharm. Biopharm*. 2017;119:28–35. V.
23. Radtke J, Kleinebudde P. Real-time monitoring of multi-layered film coating processes using Raman spectroscopy. *Europ J Pharm Biopharm*. 2020;153:43–51.
24. Romero-Torres S, Pérez-Ramos JD, Morris KR, Grant ER. Raman spectroscopic measurement of tablet-to-tablet coating variability. *J Pharm Biomed Anal*. 2005;38:270–274.
25. Müller J, Knop K, Thies J, Uerpmann C, Kleinebudde P. Feasibility of Raman spectroscopy as PAT tool in active coating. *Drug Dev Ind Pharm*. 2010;36:234–243.
26. Springer Handbook of Advanced Catalyst Characterization. In: Wachs IE, Bañares MA, eds. *Springer International Publishing*. 1st ed. Cham: Springer; 2023.
27. Kessler W, ed. *Multivariate datenanalyse: Für die pharma-, bio- und prozessanalytik: Ien Lehrbuch /Waltraud Kessler*. Weinheim: Wiley-VCH; 2007.
28. Arwa S. El Hagrasy, Shih-Ying Chang, Divyakant Desai, and San Kiang, Raman spectroscopy for the determination of coating uniformity of tablets: assessment of product quality and coating pan mixing efficiency during scale-up. 2006.
29. Deng B-C, Yun Y-H, Liang Y-Z, et al. A new strategy to prevent over-fitting in partial least squares models based on model population analysis. *Anal. Chim. Acta*. 2015;880:32–41.
30. Cramer RD. Partial Least Squares (PLS): its strengths and limitations. *Persp Drug Disc Des*. 1993;1:269–278.
31. Kriesten E, Mayer D, Alsmeyer F, Minnich CB, Greiner L, Marquardt W. Identification of unknown pure component spectra by indirect hard modeling. *Chemom Intell Labor Syst*. 2008;93:108–119.
32. Barton B, Thomson J, Lozano Diz E, Portela R. Chemometrics for Raman spectroscopy harmonization. *Appl Spectrosc*. 2022;76:1021–1041.

33. Meyer-Kirschner J, Mitsos A, Viell J. Polymer particle sizing from Raman spectra by regression of hard model parameters. *J Raman Spectroscopy*. 2018;49:1402–1411.
34. Meyer-Kirschner J, Kather M, Pich A, et al. In-line monitoring of monomer and polymer content during microgel synthesis using precipitation polymerization via raman spectroscopy and indirect hard modeling. *Appl Spectrosc*. 2016;70:416–426.
35. Echtermeyer A, Marks C, Mitsos A, Viell J. Inline Raman spectroscopy and indirect hard modeling for concentration monitoring of dissociated acid species. *Appl Spectrosc*. 2021;75:506–519.
36. Kriesten E, Alsmeyer F, Bardow A, Marquardt W. Fully automated indirect hard modeling of mixture spectra. *Chemom Intell Labor Syst*. 2008;91:181–193.
37. Alsmeyer Frank, Koß Hans-Jürgen, Marquardt Wolfgang. Indirect spectral hard modeling for the analysis of reactive and interacting mixtures. *Appl Spectrosc, AS*. 2004;58:975–985.
38. Fateixa S, Mulandeza O, Nogueira HI, Trindade T. Raman imaging studies on the stability of Paracetamol tablets under different storage conditions. *Vib Spectrosc*. 2023;124:103488.
39. Behrens G, Kuhn LT, Ubic R, Heuer AH. Raman Spectra of vateritic calcium carbonate. *Spectros Lett*. 1995;28:983–995.
40. Dreu R, Toschkoff G, Funke A, et al. Evaluation of the tablets' surface flow velocities in pan coaters. *Europ J Pharm Biopharm*. 2016;106:97–106.
41. Agarwal UP, Ralph SA, Baez C, Reiner RS. Detection and quantitation of cellulose II by Raman spectroscopy. *Cellulose*. 2021;28:9069–9079.